

Glacial expansion of oxygen-depleted seawater in the eastern tropical Pacific

Citation for published version:

Hoogakker, BAA, Lu, Z, Umling, N, Jones, L, Zhou, X, Rickaby, REM, Thunell, R, Cartapanis, O & Galbraith, E 2018, 'Glacial expansion of oxygen-depleted seawater in the eastern tropical Pacific', *Nature*, vol. 562, no. 7727, pp. 410-413. <https://doi.org/10.1038/s41586-018-0589-x>

Digital Object Identifier (DOI):

[10.1038/s41586-018-0589-x](https://doi.org/10.1038/s41586-018-0589-x)

Link:

[Link to publication record in Heriot-Watt Research Portal](#)

Document Version:

Peer reviewed version

Published In:

Nature

General rights

Copyright for the publications made accessible via Heriot-Watt Research Portal is retained by the author(s) and / or other copyright owners and it is a condition of accessing these publications that users recognise and abide by the legal requirements associated with these rights.

Take down policy

Heriot-Watt University has made every reasonable effort to ensure that the content in Heriot-Watt Research Portal complies with UK legislation. If you believe that the public display of this file breaches copyright please contact open.access@hw.ac.uk providing details, and we will remove access to the work immediately and investigate your claim.

Title: Glacial expansion of oxygen depleted seawater in the eastern tropical Pacific

Authors: Babette, A.A. Hoogakker^{1,2*}, Zunli Lu^{3,4*}, Natalie Umling⁵, Luke Jones², Xiaoli Zhou⁶, Ros E.M. Rickaby², Robert Thunell^{5¶}, Olivier Cartapanis⁷, Eric Galbraith^{8,9}.

Affiliations:

* Corresponding authors, ¶ deceased

¹ The Lyell Centre, Heriot-Watt University, Research Avenue South, EH14 4AP, Edinburgh, UK.

² Department of Earth Sciences, University of Oxford, South Parks Road, OX1 3AN, Oxford, UK.

³ Department of Earth Sciences, 310 Heroy Geology Laboratory, Syracuse University, Syracuse, NY 13244-1070 USA.

⁴ State Key Laboratory of Marine Environmental Science, Xiamen University, Xiamen 361102, China.

⁵ School of Earth, Ocean and Environment, University of South Carolina, 701 Sumter Street, EWS 617, Columbia, SC 29208 USA.

⁶ Department of Marine and Coastal Sciences, Rutgers University, 71 Dudley Rd, New Brunswick, NJ 08901, USA

⁷ University of Bern, Oeschger Centre for Climate Change Research, Falkenplatz 16, CH-3012 Bern, Switzerland.

⁸ Institut de Ciència i Tecnologia Ambientals (ICTA) and Department of Mathematics, Universitat Autònoma de Barcelona, Carrer de les Columnes, 08193 Bellaterra, Spain.

⁹ ICREA, Pg. Lluís Companys 23, 08010 Barcelona, Spain

Increased storage of carbon in the oceans has been proposed as a mechanism to explain lower atmospheric CO₂ concentrations during ice ages, yet unequivocal signatures of this storage have proven elusive¹. In seawater, the dissolved gases oxygen and carbon dioxide are linked via the production and decay of organic material such that reconstructions of low oxygen concentrations in the past indicate an increase of biologically-mediated carbon storage. Marine sediment proxy records have suggested that oxygen concentrations in the deep ocean were indeed lower during the last ice age, but that near-

33 surface and intermediate waters of the Pacific Ocean, a large fraction of which are
34 poorly-oxygenated at present, were generally better-oxygenated during the glacial¹⁻³.
35 This vertical opposition could imply a minimal net basin-integrated change in carbon
36 storage. Here we apply a novel dual-proxy approach, incorporating qualitative upper
37 water-column and quantitative bottom water oxygen reconstructions^{4,5}, to constrain
38 changes in the vertical extent of low oxygen waters in the eastern tropical Pacific since
39 the last ice age. Our tandem proxy reconstructions provide evidence of a downward
40 expansion of oxygen depletion in the eastern Pacific during the last glacial, with no sign
41 of greater oxygenation in the upper reaches of the water column. We extrapolate our
42 quantitative deep oxygen reconstructions to show that the glacial Pacific respired carbon
43 reservoir was substantially increased, establishing it as an important component of the
44 coupled mechanism that led to low glacial atmospheric CO₂.

45
46 The modern-day Pacific Ocean contains a vast volume of oxygen-depleted waters. In the
47 eastern basin, north of 18°S, waters deeper than 1 km (deepening to 2 km north of the equator)
48 are generally oxic ([O₂] > 120 μmol/kg), whereas above this most waters are hypoxic ([O₂] < 60-
49 120 μmol/kg), and a small fraction are suboxic ([O₂] < 2 to 10 μmol/kg)⁶. The eastern tropical
50 North Pacific (ETNP) oxygen minimum zone (OMZ) is the world's largest OMZ, currently
51 encompassing 67% of total suboxic waters⁶. Low oxygen conditions place important
52 limitations on marine life with hypoxic conditions proving lethal for more than half of marine
53 benthic animal species⁷. Oceanic nutrient cycling is also affected by suboxic conditions^{8,9},
54 under which remineralization of organic material occurs via anaerobic metabolic pathways,
55 including denitrification and anammox. This removes bioavailable nitrogen (which supports
56 primary production) from the ocean and generates the greenhouse gas N₂O.

Because of the intrinsic link between oxygen and carbon during photosynthesis and respiration, oxygen utilization provides a direct reflection of the strength of the biological carbon pump and therefore its influence on atmospheric CO₂⁴. Today the Pacific Ocean represents the largest modern sink of respired organic carbon (>730 Gt, ~50% of the global ocean inventory¹⁰), half of which resides in the upper 1.5 km.

The concentration of dissolved oxygen in seawater is controlled by (i) the saturation oxygen concentration of seawater in contact with the atmosphere, which is the sum of oxygen solubility (a function of temperature and salinity) and any disequilibrium from saturation at the ocean surface, and (ii) net oxygen utilization, which is determined by the accumulated consumption during remineralization of organic material along the pathways of advection and mixing⁸. Over the last 50 years an observed vertical expansion of the equatorial Pacific OMZ has been attributed mostly to a net increase of oxygen utilization, which could reflect a reduced input rate of oxygen through advection and mixing and/or an increase in the local rate of organic matter respiration^{11,12}. A further decline in ocean oxygen levels is predicted by Earth system models under anthropogenic warming, linked to increased temperatures (lowering saturation oxygen concentration) and increased oxygen utilization due to decreased ventilation^{8,11,13}. However, model simulations disagree about oxygen changes in the tropical thermoclines, and do not reproduce the large historical changes¹¹, suggesting these models are missing important processes that may compromise their predictions of future change^{13,14}.

Reconstructions of the last ice age offer an alternative test of the link between climate and ocean oxygenation. Lower glacial seawater temperatures would have increased oxygen saturation concentrations² and decreased remineralization rates¹⁵. These conditions could have resulted in a better oxygenated upper ocean, potentially eliminating the OMZs. Bulk sedimentary nitrogen isotope ($\delta^{15}\text{N}$) records from the eastern tropical Pacific (ETP)^{16,17} have been interpreted to reflect overall reduced glacial denitrification rates in the upper water

column¹⁸, which could indicate an absence of suboxic waters. In contrast, the cold-enhanced solubility appears to have been overwhelmed by increased oxygen utilization in the deep Pacific, resulting in reduced oxygen concentrations and increased respired carbon storage that could have contributed to the low atmospheric CO₂ concentrations¹⁻³. However, these reconstructions are based on qualitative proxies, which are often difficult to interpret¹⁹. Furthermore, many of these records have been limited to core sites from continental slopes, and are potentially biased by local conditions¹⁹.

To constrain upper-water column oxygen concentrations, we utilized planktonic foraminifera I/Ca⁵. This proxy takes advantage of iodine speciation in seawater. The iodate species (IO₃⁻) is favoured under well-oxygenated settings, whereas iodide (I⁻) becomes the dominant species under oxygen-depleted conditions. Foraminiferal calcite only incorporates iodate, so that foraminiferal I/Ca reflects the abundance of the oxidised form²⁰.

Furthermore, we utilize the benthic foraminiferal carbon isotope gradient proxy ($\Delta\delta^{13}\text{C}$) to quantitatively reconstruct bottom water oxygen concentrations⁴. The $\Delta\delta^{13}\text{C}$ between bottom water and pore-water at the anoxic boundary in sediments is related to the oxygen concentration of the overlying bottom waters²¹. The $\Delta\delta^{13}\text{C}$ between bottom water and pore-water at the anoxic boundary is reproduced by the $\Delta\delta^{13}\text{C}$ of benthic foraminifera with microhabitats in bottom water (*Cibicidoides wuellerstorfi*) and in sediments at the anoxic boundary (*Globobulimina spp.*)⁴. This method allows us to quantitatively reconstruct past dissolved oxygen concentrations in the range of 55 to 235 $\mu\text{mol/kg}$ (see methods) in bottom waters from tropical to temperate regions, with an estimated total standard error of 17 $\mu\text{mol/kg}$ ⁴. Our tandem proxy approach allows us to place firm constraints on past changes in the geometry of oxygen depleted waters in the eastern tropical Pacific over the last 40,000 years. Furthermore, extrapolation of our new quantitative bottom water oxygen reconstructions allows us to

calculate the change in the size of the Pacific respired carbon pool and assess its role in glacial-interglacial CO₂ cycles.

Planktonic foraminifera I/Ca ratios were measured at two eastern tropical Pacific sites. Site ODP 1242 (7.86°N, 83.61°W, 1.36 km) is on the Costa Rica margin, in the eastern tropical North Pacific (ETNP), while ODP 849 (0.18°N, 110.50°W, 3.85 km) lies beneath the eastern equatorial cold tongue (Fig. 1). Planktonic foraminifera I/Ca ratios at the ETNP site are expected to monitor changes in the upper boundary of the ETNP-OMZ. The cold tongue Site ODP 849 is distal from modern suboxic zones but downstream of waters that have passed through them, and planktonic foraminifera I/Ca ratios at this location are expected to have responded to the broader presence of oxygen depleted waters within the ETP-OMZ. The location of ODP 1242 at the deep boundary of the present day ETNP-OMZ is ideal to test for changes in the vertical extent of the OMZ, via benthic foraminifera $\Delta\delta^{13}\text{C}$. Additionally, bottom water oxygen concentrations were reconstructed for deep water at TR163-25 (1.65°S, 88.45°W, 2.65 km), to provide quantitative estimates of changes in deep water oxygen concentrations in the eastern tropical Pacific and calculate the glacial increase in the deep Pacific respired carbon pool. Details of age models are provided in the methods section (EDtables 1, 2, EDfig 4).

Modern oxygen profiles at ODP Sites 849 and 1242 are very similar (Fig. 1), except that OMZ waters ([O₂] threshold < 45 $\mu\text{mol/kg}^{23}$) occur at a much shallower depth (within the upper 50 m) at the ETNP site compared to the cold tongue site (deeper than 250 m) (Fig. 1). This upper water column difference is consistent with the contrasting core-top planktonic foraminifera I/Ca values at the two sites (Fig. 2). If suboxia had been reduced during the glacial, as has been previously argued, one would expect high I/Ca to be found in glacial-age foraminifera. Instead we find that low I/Ca (<0.6 $\mu\text{mol/mol}$) prevailed continuously over the last 40 kyrs at the ETNP-OMZ site, consistent with persistent oxygen depletion at shallow depths (Fig. 2).

Furthermore, although I/Ca ratios of all planktonic species in the cold tongue from 40-25 ka BP were similar to late Holocene values, during early deglaciation (~18-16 ka BP) the I/Ca of shallow dwelling species fell to values as low as the thermocline species. Persistently depleted planktonic foraminifera oxygen isotopes values of the shallow dwelling species and heavy values of the thermocline species (Fig. 2) indicate similar depth habitats over the last 40 kyrs. Therefore, the lower I/Ca values of the shallow dwelling species at Site 849 during early deglaciation are interpreted to be due to an increased presence of oxygen-depleted waters in the ETP-OMZ.

Turning to the deep sea, reconstructed dissolved oxygen at ODP Site 1242 shows generally lower concentrations during the glacial compared to the Holocene, with an average LGM (18 to 22 ka BP) dissolved oxygen content of 55 $\mu\text{mol/kg}$ ($\pm 17 \mu\text{mol/kg}$, Fig. 3). The lowest oxygen concentrations (44 $\mu\text{mol/kg}$) were recorded during early deglaciation, (17 to 15 ka BP), followed by a rapid increase in the mid-late deglaciation. Maximum oxygen concentrations of 100 $\mu\text{mol/kg}$ were recorded during the early Holocene. Oxygenation then decreased slightly through the Holocene, reaching late Holocene values of 85 $\mu\text{mol/kg}$ (Fig. 3). At the deeper site TR163-25, reconstructed LGM oxygen concentrations are similar to ODP Site 1242, averaging 54 $\mu\text{mol/kg}$ (Fig. 3), and there is also a brief decline in dissolved oxygen during the early deglaciation to ~40 $\mu\text{mol/kg}$ followed by a rapid increase to ~160 $\mu\text{mol/kg}$ in the mid-Holocene (Fig. 3).

Our dual-proxy results from the upper 1.4 km of the water column (planktonic foraminifera I/Ca at ODP Sites 1242 & 849, $\Delta\delta^{13}\text{C}$ at ODP Site 1242) show sustained oxygen depletion in contrast with other studies that have suggested the upper water column in the Pacific was generally more oxygenated at this time¹⁻³. These prior conclusions were based on observations of low sedimentary $\delta^{15}\text{N}$ (interpreted as lower rates of denitrification), weaker sedimentary laminations and lower oxygen-sensitive trace metal abundances during the glacial². However,

as we explain in our method section (e.g. see EDfig. 5) there are several reasons that sedimentary $\delta^{15}\text{N}$ could have been lower during the glacial without a significant change in oxygen concentrations. Furthermore, the sedimentary laminations and trace metals previously examined at three sites in the coastal ETP showed only weak signs of oxygen change between the LGM and Holocene^{16,17}, which could also be attributed to changes in the characteristics of accumulating sediments^{26,27}. Thus, the persistently low I/Ca values, in combination with lowered glacial bottom water oxygen levels at 1.4 km (today the lower boundary of the ETNP-OMZ), do not support a significant contraction of the upper reaches of the tropical Pacific OMZ during the glacial period compared to today.

Our results also indicate a period of particularly strong oxygen depletion during the early deglaciation, consistent with prior sedimentary $\delta^{15}\text{N}$, lamination, and trace metal evidence from the ETNP^{16,17}. The convergence of mixed layer and thermocline planktonic foraminifera to low values of I/Ca at ODP Site 849 (Fig. 2) suggests that the downward expansion of oxygen depleted waters in the ETP-OMZ, indicated by the bottom water oxygen reconstructions (Fig. 3), was accompanied by an intensified influence of oxygen depleted-waters in the upper water column. The interval coincides with a weak Atlantic Meridional Overturning Circulation, and an apparent productivity peak in the eastern equatorial Pacific speculated to reflect increased delivery of nutrients from southern-sourced deep waters and intensified upwelling^{17,28-30}.

Our tandem proxy results provide new insights into the evolution of respired carbon storage in the eastern tropical Pacific since the last ice age. Today half of the total global respired carbon reservoir is stored in intermediate and subsurface waters of the Pacific (e.g. upper 1.5 km). Our results suggest little LGM-Holocene change in the respired carbon reservoir of the upper water column, but an increase of the deeper Pacific respired reservoir, implying a net increase in the size of the Pacific glacial respired pool.

Furthermore, our $\Delta\delta^{13}\text{C}$ results show that the modern vertical oxygen gradient ($\Delta[\text{O}_2]$ of ~ 65 $\mu\text{mol/kg}$) between water depths of 1.4 and 2.6 km was eliminated during the LGM (Fig 1), so that oxygen concentrations did not increase with depth as they do today. We also find that the gradient in $\delta^{13}\text{C}$ of DIC between these water masses was reversed (methods EDfig. 6), as would be expected given the respired carbon concentrations inferred from our quantitative oxygen reconstructions, and similar changes in the preformed component of $\delta^{13}\text{C}$ (for details see Methods). Our data therefore suggest that, despite large changes in average $\delta^{13}\text{C}$ of DIC for the whole ocean and changes in air-sea exchange, the relative change in $\delta^{13}\text{C}$ between sites in the 1.4 - 3 km depth range provides a good approximation of oxygen change.

We take advantage of this new constraint together with our LGM-modern $\delta^{13}\text{C}$ compilation to extrapolate our results spatially in the deep Pacific. Our results suggest that the total amount of respired carbon in the Pacific increased by roughly 90 Gt C between water depths of 1.4 and 3 km, and possibly 200 Gt C across the whole of the deep Pacific (Methods). This provides a useful new target for model simulations of glacial carbon cycling. Whilst the average increase in respired carbon concentrations in deeper waters of the Pacific is only half that of the deep Atlantic⁴, the estimated glacial increase in its respired carbon reservoir is almost three times that of the deep Atlantic due to its vast size. This suggests that the Pacific made an important contribution to glacial-interglacial changes in atmospheric CO_2 levels.

References:

1. Sigman, D.M., Boyle, E.A. Glacial/interglacial variations in atmospheric carbon dioxide. *Nature* **407**, 859-869 (2000).

2. Galbraith, E.D., Jaccard, S.L. Deglacial weakening of the oceanic soft tissue pump:
global constraints from sedimentary nitrogen isotopes and oxygenation proxies.
Quaternary Sci. Rev. **109**, 38-48 (2015).
3. Bradtmiller, L.I., Anderson, R.F., Sachs, J.P., Fleisher, M.Q. A deeper respired carbon
pool in the glacial equatorial Pacific Ocean. *Earth Planet. Sc. Lett.* **299**, 417-425 (2010).
4. Hoogakker, B.A.A., Elderfield, H., Schmiedl, G., McCave, I.N., Rickaby, R.E.M.
Glacial-interglacial changes in bottom-water oxygen content on the Portuguese margin.
Nat. Geosci. **8**, 40-43 (2015).
5. Lu, Z., Hoogakker, B.A.A., Hillenbrand, C.-D., Zhou, X., E. Thomas, E., et al. Oxygen
depletion recorded in upper waters of the glacial Southern Ocean. *Nat. Comm.* **7**, 11146
(2016).
6. Bianchi, D., Dunne, J.P., Sarmiento, J.L., Galbraith, E.D. Data-based estimates of
suboxia, denitrification, and N₂O production in the ocean and their sensitivities to
dissolved O₂. *Glob. Biogeochem. Cycles* **26**, doi:10.1029/2011GB004209 (2012).
7. Vaquer-Sunyer, R., Duarte, D.M. Thresholds of hypoxia for marine biodiversity. *PNAS*
105, 14352-15457 (2008).
8. Keeling, R., Körtzinger, A., Gruber, N. Ocean deoxygenation in a warming world. *Annu.*
Rev. Mar. Sci. **2**, 199-229 (2010).
9. Lam, P., Kuypers, M.M.M. Microbial nitrogen cycling processes in oxygen minimum
zones. *Annu. Rev. Mar. Sci.* **3**, 317-345 (2011).
10. Schmittner, A., Somes, C.J. Complementary constraints from carbon (¹³C) and nitrogen
(¹⁵N) isotopes on the glacial ocean's soft-tissue biological pump. *Paleoceanography* **31**,
669-693 (2016).

11. Schmidtko, S., Stramma, L., Visbeck, M. Decline in global oceanic oxygen content during the past five decades. *Nature* **542**, 335-229 (2017).
12. Stramma, L., Johnson, G.C., Sprintall, J., Mohrholz, V. Expanding oxygen-minimum zones in the tropical oceans. *Science* **320**, 656-658 (2008).
13. Bopp, L., Resplandy, L., Orr, J.C., Doney, S.C., Dunne, J.P., Gehlen, M., Halloran, P., Heinze, C., Ilyina, T., Séférian, R., Tjiputra, J., Vichi, M. Multiple stressors of ocean ecosystems in the 21st century: projections with CMIP5 models. *Biogeosciences* **10**, 6225-6245 (2013).
14. Long, M., Deutsch, C., Ito, I. Finding forced trends in oceanic oxygen. *Glob. Biogeochem. Cycles* **30**, 318-397 (2016).
15. Matsumoto, K. Biology-mediated temperature control on atmospheric pCO₂ and ocean biogeochemistry. *Geophys. Res. Lett.* **34**, doi:10.1029/2007GL031301 (2007).
16. Pichevin, L.E., Ganashram, R.S., Francavilla, S., Arellano-Torres, E., Pedersen, T.F., Beaufort, L. Interhemispheric leakage of isotopically heavy nitrate in the eastern tropical Pacific during the last glacial period. *Paleoceanography* **25**, PA1204 (2010).
17. Hendy, I.L., Pedersen, T.F. Oxygen minimum zone expansion in the eastern tropical North Pacific during deglaciation. *Geophys. Res. Lett.* **33**, L20602 (2006).
18. Galbraith, E.D., Kienast, M., and the NICOPP working group members. The acceleration of ocean denitrification during deglacial warming. *Nat. Geosci.* **6**, 579-584 (2013).
19. Moffit, S.E., Moffit, R.A., Sauthoff, W., Davis, C.V., Hewett, K., Hill, T.M. Paleoceanographic insights on recent oxygen minimum zone expansion: lessons for modern oceanography. *PLoS ONE* **10**, doi:10.1371/journal.pone.0115246 (2015).

20. Lu, Z., Jenkyns, H.C., Rickaby, R.E.M. Iodine to calcium ratios in marine carbonates as a paleo-redox proxy during oceanic anoxic events. *Geology* 38, 1107-1110 (2010).
21. McCorkle, D.C., Emerson, S.R. The relationship between pore water carbon isotopic composition and bottom water oxygen concentration. *Geochim. Cosmochim. Acta* **52**, 1169-1178 (1988).
22. Garcia, H., Boyer, T.P., Locarnini, R.A., Antonov, J., Mishonov, A.V., Baranova, O., Zweng, M.M., Reagan, R.J., Johnson, D.R., Levitus, S. *World ocean atlas 2013. Volume 3, dissolved oxygen, apparent oxygen utilization, and oxygen saturation*. In Levitus S. (Ed.) NOAA Atlas NESDIS 75, U.S. Government Printing Office, Washington, D.C. **27 pp.** (2013).
23. Karstensen, J., Stramma, L., Visbeck, M. Oxygen minimum zones in the eastern tropical Atlantic and Pacific oceans. *Prog. Oceanogr.* 77, 331-350 (2008).
24. Stern, J.V., Lisiecki, L.E. Termination 1 timing in radiocarbon-dated regional benthic $\delta^{18}\text{O}$ stacks. *Paleoceanography* **29**, 1127-1142 (2014).
25. Benway, H.M., Mix, A.C., Haley, B.A., Klinkhammer, G.P. Eastern Pacific warm pool paleosalinity and climate variability: 0-30 kyr. *Paleoceanography* **21**, PA3008 (2006).
26. van Geen, A., Zheng, Y., Bernhard, M., Cannariato, K.G., Carriguiry, J., Dean, W.E., Eakins, B.W., Ortiz, J.D., Pike, J. On the preservation of laminated sediments along the western margin of North America. *Paleoceanography* **18**, doi:10.1029/2003PA000911 (2003).
27. Nameroff, T.J., Calvert, E., Murray, J.W. Glacial-interglacial variability in the eastern tropical North Pacific oxygen minimum zone recorded by redox-sensitive trace metals. *Paleoceanography* **19**, doi:10.1029/2003PA000912 (2004).

28. Costa, K.M., Jacobel, A.W., McManus, J.F., Anderson, R.F., Winckler, G., Thiagarajan,
N. Productivity patters in the Equatorial Pacific over the last 30,000 years. *Glob.*
Biogeochem. Cycles **31**, 850-865 (2017).
29. Kienast, M., Kienast, S.S., Calvert, S.E., Eglinton, T.I., Mollenhauer, G., Francois, R.,
Mix, A.C. Eastern Pacific cooling and Atlantic overturning circulation during the last
deglaciation. *Nature* **443**, 846-849.
30. de la Fuente, M., Skinner, L., Calvo, E., Pelejero, C., Cacho, I. Increased reservoir ages
and poorly ventilated deep waters inferred in the glacial Eastern Equatorial Pacific. *Nat.*
Comm. **6**, 7420 (2015).

Acknowledgments: This work benefitted greatly from discussions with Raja Ganeshram. This
work is supported by UK Natural Environment Research Council (NERC) grant
NE/I020563/1 (to BAAH) and National Science Foundation (NSF) OCE-1232620,
OCE-1736542 (to ZL). This research used samples and/or data provided by the Ocean
Drilling Program (ODP). ODP is sponsored by the U.S. National Science Foundation
and participating countries (Natural Environment Research Council in UK) under
management of Joint Oceanographic Institutions (JOI), Inc. Mike Hall, James Rolfe
(University of Cambridge) and Chris Day (University of Oxford) are thanked for help
with stable isotope analyses.

Author contributions: BAAH and ZL conceived and coordinated the work. BAAH, ZL, NU,
LJ, XZ carried out data analyses; OC carried out data synthesis. BAAH, ZL and EG
constructed the figures and wrote the paper, with contributions from the other co-
authors.

Author Information: Reprints and permissions information is available at
www.nature.com/reprints. The authors declare no competing financial interests. Readers are
welcome to comment on the online version of the paper. Data is available from
https://doi.pangaea.de/10.1594/PANGAEA.891185. Correspondence should be addressed to
BH or ZL (b.hoogakker@hw.ac.uk or zunlilu@syr.edu).

Figure captions

Figure 1. Overview of dissolved oxygen concentrations ($[O_2]$) in the eastern Pacific Ocean.

a, between 60°S and 60°N at 400 m water depth (circles show core locations). Data are from²². **b**, vertical profiles at the core sites (from <https://www.nodc.noaa.gov/OC5/SELECT/dbsearch/dbsearch.html>) Data are from²².): ODP Site 1242 (dark green), ODP Site 849 (black) and TR163-25 (light green). Note different scale for upper part (0-1000 m) and lower part (1000-4000 m) of the water column. Arrows on the x-axis indicate $[O_2]$ thresholds for suboxia (light grey) and the OMZ (dark grey). Diamonds illustrate reconstructed LGM bottom water $[O_2]$ values at ODP Site 1242 and TR163-25, including $\pm 17 \mu\text{mol/kg}$ error⁴.

Figure 2. Reconstructed ETP surface water oxygenation. **a**, planktonic foraminiferal and benthic composite oxygen isotope ($\delta^{18}\text{O}$) records (blue symbols) and stacked records (grey lines)²⁴ at ODP Sites 849 and 1242. Planktonic foraminiferal oxygen isotopes at 1242 until 28 ka BP are from²⁵. Details of age models can be find in the methods section. **b**, I/Ca ratios of planktonic foraminifera. I/Ca ratios $< 2.5 \mu\text{mol/mol}$ are indicative of the presence of low oxygen waters in the upper 400 m of the water column⁵.

Figure 3. Reconstructed ETP bottom water oxygen concentrations. **a**, benthic foraminiferal $\delta^{18}\text{O}$ (blue symbols) of ODP Site 1242 and TR163-25 (*C. wuellerstorfi*, adjusted by +0.64‰) and stacked records (grey lines) from the intermediate and deep Pacific²⁴. Details of age models can be find in the methods section. **b**, benthic foraminiferal carbon isotopes of *C. wuellerstorfi* (red) and spp. *Globobulimina* (blue). **c**, reconstructed bottom water $[O_2]/\Delta\delta^{13}\text{C}$ (raw data black squares + total error of $\pm 17 \mu\text{mol/kg}$ ⁴, thick line shows moving average calculated using the boxcar algorithm). Yellow boxes: modern range of bottom water oxygen concentrations.

METHODS

Analytical methods

Foraminifera oxygen and carbon isotopes for ODP Site 849 and 1242 were measured using a Thermo MAT253 IRMS coupled to a Kiel Device at the Godwin Laboratory (University of Cambridge) and a Thermo Delta V Advantage coupled to a Kiel Device at the Department of Earth Sciences (University of Oxford). Calibration to VPDB was via NBS19 standards. Overall precision for $\delta^{18}\text{O}$ is $\sigma=0.07\text{‰}$ (Oxford) and $\sigma=0.08\text{‰}$ (Cambridge), and for $\delta^{13}\text{C}$ is $\sigma=0.04\text{‰}$ (Oxford) and $\sigma=0.06\text{‰}$ (Cambridge). For benthic foraminifera analyses we typically used 3-5 specimens of *C. wuellerstorfi*, 6 specimens of *C. pachyderma*, and > 4 specimens of *Globobulimina* spp. For planktonic foraminifera analyses a minimum of 20 specimens were analysed. For site TR163-25 benthic foraminifera oxygen and carbon isotopes, as well as (homogenized) bulk sedimentary nitrogen isotopes, were measured on a GV Isoprime stable isotope ratio mass spectrometer at the University of South Carolina, with a long-term lab reproducibility of 0.07‰ (oxygen) 0.06‰ (carbon), and 0.14‰ (nitrogen). Typically 1-5 *Globobulimina* spp. and *C. wuellerstorfi* were used for benthic foraminifera stable isotope analyses at site TR163-25.

Planktonic foraminifera I/Ca ratios were measured by quadrupole ICP-MS (Bruker M90) at Syracuse University, using the method of⁵. The sensitivity of iodine was tuned to above 80 kcps for a 1 p.p.b. standard. Iodine calibration standards were freshly prepared from KIO₃ powder. The precision for ¹²⁷I is typically better than 1%. The detection limit of I/Ca is on the order of 0.1 $\mu\text{mol/mol}$.

346

347 **Age models**

348 The age models for ODP 849 and 1242 are based on oxygen isotope stratigraphy, matching
349 new benthic foraminiferal $\delta^{18}\text{O}$ records (EDFig. 1, EDtable 1) to the Pacific intermediate and
350 deep stacked $\delta^{18}\text{O}$ records of Stern and Lisiecki²⁴. The benthic composite $\delta^{18}\text{O}$ record of ODP
351 Site 849 features specimens of *C. wuellerstorfi*, *Laticarinina pauperata* (both adjusted by
352 +0.64‰ to bring it closer to values of *Uvigerina* spp.), and *Uvigerina* spp. The composite
353 record of ODP Site 1242 $\delta^{18}\text{O}$ includes mainly specimens of *C. wuellerstorfi*, *Cibicidoides*
354 *pachyderma* (both adjusted by +0.64‰), and minor *Uvigerina peregrina*.

355

356 For TR163-25 the chronology was developed using 1 *G. ruber* and 3 *N. dutertrei* ^{14}C ages
357 (EDtable 2) calibrated with reservoir ages calculated for the EEP from TR163-23³¹ and
358 ODP1240³⁰ using the Bayesian age model program BACON³².

359

360 **Bottom water oxygen concentrations**

361 Hoogakker et al.⁴ show there is a strong ($R^2 = 0.94$) linear relationship between bottom water
362 oxygen concentrations and $\Delta\delta^{13}\text{C}$ at oxygen levels between 55 and 235 $\mu\text{mol/kg}$, with a $\sim 0.4\text{‰}$
363 increase in $\Delta\delta^{13}\text{C}$ for every 50 $\mu\text{mol/kg}$ increase in bottom water oxygen concentrations.
364 According to⁴, the total error associated with bottom water oxygen concentration at mid- to
365 low latitudes is $\pm 17 \mu\text{mol/kg}$. When oxygen concentrations exceed 255 $\mu\text{mol/kg}$, the
366 relationship with $\Delta\delta^{13}\text{C}$ weakens due to $\delta^{13}\text{C}$ of *Globobulimina* spp. becoming much more
367 depleted. This typically occurs in environments where the oxygen penetration depth is deeper
368 than the sediment mixed layer causing addition of light carbon through sulphate reduction²¹.
369 At oxygen concentrations between 50 and 20 $\mu\text{mol/kg}$ we expect the strong linear relationship

(($\Delta\delta^{13}\text{C} = 0.00772 \times [\text{dissolved oxygen concentration}] + 0.41446$) to hold, as aerobic respiration
 still dominates the remineralization of organic carbon³³. This is supported by 2 new data points
 derived from temperate North Pacific Holocene samples of ODP Sites 1014 ($[\text{O}_2] = 32 \pm 10$
 $\mu\text{mol/kg}$; $\Delta\delta^{13}\text{C} = 0.54 \pm 0.03\text{‰}$) and 1019 ($[\text{O}_2] = 21 \pm 6 \mu\text{mol/kg}$; $\Delta\delta^{13}\text{C} = 0.44 \pm 0.1\text{‰}$). At ODP
 Site 1242 one data point from ~38 ka BP fell outside of the calibration (reconstructed $[\text{O}_2]$ of
 16 $\mu\text{mol/kg}$) and is not shown in Figure 3. At ODP Site 1242, products of manganese and iron
 reduction (Mn^{2+} and Fe^{2+}) become important below 50 meters composite depth³⁴
 (reconstructions of $\Delta\delta^{13}\text{C}$ only took place between 0 and 6.5 m). Therefore, we do not expect
 deviations in $\Delta\delta^{13}\text{C}$ in relation to these processes. The most recent Holocene is missing from
 core 1242, as evidenced by high core top $\delta^{13}\text{C}$ of *C. wuellerstorfi*, (average 0.4‰ top 25 cm)
 in contrast with seawater $\delta^{13}\text{C}$ of dissolved inorganic carbon (DIC) of -0.2 to -0.3‰³⁵. At
 TR163-25 the late Holocene (< 3,500 years) is missing.

Subsurface water oxygen concentrations

To document upper ocean oxygenation, we use the planktonic foraminifera I/Ca proxy of⁵.
 The electrode potential of the iodate/iodide couple is very similar to that of denitrification³⁶. In
 the surface ocean iodide exists in well oxygenated settings, which has been attributed to
 disequilibrium caused by biological activity and photochemical reduction of iodate to iodide<sup>37-
 39</sup>. The oxidation of iodide back to iodate is slow and may take from months to up to 40 years²⁰.
 I/Ca ratios were measured on several planktonic foraminifera species covering a range of depth
 habits. Spinose species *Globigerinoides sacculifer* (ODP 849, 1242) and *G. ruber* (ODP 1242)
 typically live in the surface mixed layer, whereas non-spinose species *Pulleniatina*
obliquiloculata (ODP 849), *Globorotalia menardii* (ODP 1242), and *Neogloboquadrina*
dutertrei (ODP 849, 1242) live deeper, at or below the thermocline⁴⁰⁻⁴². These depth habitat
 differences are expressed in the oxygen isotopes records, with consistently depleted values for

the warmer surface mixed layer species, and heavier values for the deeper and cooler water dwelling species (Fig. 2). Pristine planktonic foraminifera were rigorously cleaned using the cleaning method of⁴³ prior to I/Ca analyses.

It is unlikely that lower deglacial I/Ca ratios at ODP 849 are due to productivity changes; modern open ocean productivity pulses do not lower IO_3^- to concentrations below $0.25 \mu\text{mol/l}$ in oxygenated water, suggesting that our planktonic foraminifera I/Ca signals are most likely driven by subsurface water oxygen concentrations and not productivity⁵.

Nitrogen isotopes

Bulk sedimentary $\delta^{15}\text{N}$ can indirectly reflect the extent of suboxia within the upper water column, near the core site, due to the enrichment of ^{15}N in residual nitrate during denitrification⁴⁴. Nitrogen isotopes can however also be affected by other processes such as dilution of the isotopic signal given the fraction of nitrate consumed by denitrification in suboxic zones⁴⁵, the input of nitrate by advection from distant suboxic zones¹⁶, the addition of low ^{15}N nitrogen by N_2 fixation, and partial nitrate uptake by phytoplankton at remote locations^{18, 46}, and so are not unambiguous recorders of the local extent of suboxia.

Bulk sedimentary $\delta^{15}\text{N}$ at both ODP Site 1242 and TR163-25 (EDfig. 2) show lower values during the LGM, consistent with other $\delta^{15}\text{N}$ records within the region¹⁸. Only at ODP Site 1242 are sufficiently-low oxygen concentrations ($[\text{O}_2] < 2\text{--}4 \mu\text{mol/kg}$) found for denitrification to occur today⁴⁹, and only at more than 300 m depth in the water column (Fig. 1). This is below the depth from which wind-driven upwelling draws. Thus, the nitrogen incorporated in organic matter at the surface and exported to depth, producing the bulk sedimentary $\delta^{15}\text{N}$ record, does not directly reflect local suboxia at either site. Instead, the records at these locations are likely to reflect regional changes in nitrogen cycling, as is true for the similar records found

throughout the ETP¹⁸. These changes could have included lower rates of denitrification despite similar volumes of OMZ waters, or more complete nitrate consumption during denitrification leading to a weaker isotopic signal.

Notably, nitrogen isotope values at the Gulf of Tehuantepec, where the most active water column denitrification occurs today, were similar during the LGM and late Holocene (7‰) consistent with similarly active denitrification during both times¹⁷.

Changes in the soft tissue pump

The $\delta^{13}\text{C}$ value of dissolved inorganic carbon ($\delta^{13}\text{C}_{\text{DIC}}$) depends on both the preformed component ($\delta^{13}\text{C}_{\text{pre}}$) and soft tissue components ($\delta^{13}\text{C}_{\text{soft}}$). The latter term results from the remineralization of organic matter and is related through stoichiometric ratios to oxygen consumption and carbon storage. The $\delta^{13}\text{C}_{\text{pre}}$ is determined by temperature, salinity, $p\text{CO}_2$, alkalinity, the whole ocean average $\delta^{13}\text{C}$, and the disequilibrium of surface waters when they sink. Often overlooked, the $\delta^{13}\text{C}_{\text{pre}}$ value is sensitive to changes in the soft tissue pump and ocean circulation in addition to globally-averaged $^{13}\text{C}/^{12}\text{C}$.

If we ignore the small impact of the carbonate pump on carbon isotopes, the $\delta^{13}\text{C}_{\text{DIC}}$ at an arbitrary point in the ocean interior is given by:

$$\delta^{13}\text{C}_{\text{DIC}} = (\delta^{13}\text{C}_{\text{pre}} \times \text{DIC}_{\text{pre}} + \delta^{13}\text{C}_{\text{soft}} \times \text{DIC}_{\text{soft}}) / \text{DIC}_{\text{tot}} \quad \text{eq. 1}$$

The LGM-Holocene change (D) in all quantities is approximately:

$$D\delta^{13}\text{C}_{\text{DIC(LGM-Hol)}} = D(\delta^{13}\text{C}_{\text{pre}} \times \text{DIC}_{\text{pre}}) / \text{DIC}_{\text{tot}} + D(\delta^{13}\text{C}_{\text{soft}} \times \text{DIC}_{\text{soft}}) / \text{DIC}_{\text{tot}} \quad \text{eq. 2}$$

442

443 This equation includes a number of unknowns, that can be simplified using three assumptions.

444 First, that changes in $\delta^{13}\text{C}_{\text{soft}}$ were negligible. Second, that although the shallow and deep sites

445 certainly would have had different preformed components, the glacial-interglacial change in

446 the preformed component, $D(\delta^{13}\text{C}_{\text{pre}} \times \text{DIC}_{\text{pre}})$, was the same at the two sites. Third, that the

447 change in $\text{DIC}_{\text{soft}}/\text{DIC}_{\text{tot}}$ was small. This then gives change in $\delta^{13}\text{C}_{\text{pre}}$ between the two depths

448 in (z2-z1) as:

449

450
$$D\delta^{13}\text{C}_{\text{DIC}(z2-z1)} = \delta^{13}\text{C}_{\text{soft}} \times D\text{DIC}_{\text{soft}(z2-z1)} / \text{DIC}_{\text{tot}} \quad \text{eq. 3}$$

451

452 The $\delta^{13}\text{C}_{\text{DIC}}$ data show that the relative change between the deep and shallow site changes from

453 0.2‰ during recent times to -0.3‰ during the LGM, a change of 0.5‰. Assuming $\delta^{13}\text{C}_{\text{soft}}$ is -

454 23‰ and DIC is about 2200,

455

456
$$-0.5 = (-23) \times (D\text{DIC}_{\text{soft}} / 2200)$$

457

458
$$\Delta \text{DIC}_{\text{soft}} = 48$$

459

460 This would imply a glacial-interglacial relative change in oxygen utilization between the two

461 depths of $48 * 140 [\text{O}_2] / 106 \text{ C} = 63 \mu\text{M}$. Our new reconstructions show that oxygen

462 concentrations at the two depths converged at the LGM. At present, oxygen concentrations at

463 the deeper site are ~65 μM higher than the shallow site, which would imply that, based on the

464 $\delta^{13}\text{C}$, oxygen concentrations during the LGM should have been the same at the two sites. This

465 is essentially what we observe, supporting the assumption of similar changes in the preformed

components in the waters bathing the two depths. Note that this is not to say that the preformed components were constant. Rather, they both changed considerably, but in a coordinated way, due to the whole ocean change of 0.34‰, and complex interconnected changes in temperature, alkalinity, salinity, pCO_2 and air-sea exchange dynamics. Because those changes appear to have occurred in concert at these depths, we can then take the assumption that, for the Pacific between ~1-3 km depth, there was a uniform LGM-recent change in $\delta^{13}C_{pre}$. As a result, the relative changes in $\delta^{13}C$ between sites should have been dominated by DIC_{soft} changes, allowing a large-scale budget to be constructed.

Between 1.4 and 3 km the average LGM-Recent $\delta^{13}C$ of DIC difference is $-0.10 \pm 0.13\text{‰}$. At TR163-25, LGM-Recent $\delta^{13}C$ was -0.30‰ , while dissolved oxygen values were decreased by 65 $\mu\text{mol/kg}$ compared with recent times (EDfig3). Thus, with our new constraints, the average decrease of 0.10‰ in LGM-Recent $\delta^{13}C$ of DIC between 1.4 and 3 km in the Pacific can be translated to oxygen concentrations that were 22 $\mu\text{mol/kg}$ lower $((-0.10/0.30)*65)$ than preindustrial (not accounting for changes in preformed oxygen disequilibrium). Assuming a 2.5 °C decrease in average deep Pacific temperature and a 1 unit increase in salinity (e.g. ⁵¹), the saturated dissolved oxygen concentration (calculated using the equations of ⁵²) would be 353 $\mu\text{mol/kg}$, nearly 20 $\mu\text{mol/kg}$ higher than at present. Apparent oxygen utilization (difference between saturation oxygen concentration and measured oxygen concentration) was therefore increased by 42 $\mu\text{mol/kg}$ during the LGM in the deep Pacific. Extrapolated across water depths between 1.4 and 3 km this amounts to an increase in respired carbon of 90 Gt C. If similar conditions and changes in $\delta^{13}C_{pre}$ applied across the whole of the deep Pacific (all depths > 1.4 km), a volume over which the average LGM-Recent $\delta^{13}C$ is $-0.17 \pm 0.18\text{‰}$, then the corresponding increase in respired carbon would amount to 200 Pg C.

References METHODS:

31. Umling, N.E., Thunell, R.C. Synchronous deglacial thermocline and deep-water ventilation in the eastern equatorial Pacific. *Nat. Comm.* **8**, 14203 (2017).
32. Blaauw, M., Christen, J.A. Flexible paleoclimate age-depth models using an autoregressive gamma process. *Bayesian Anal.* **6**, 457-474 (2011).
33. Codispotti, L., Yoshinari, T., Devol, A.H. Suboxic respiration in the oceanic water column. In: *Respiration in Aquatic Ecosystems*, doi:10.1093/acprof:oso/9780198527084.001.0001 (2005).
34. Mix, A.C., Tiedemann, R., Blum, P., et al. *Proc. ODP Init. Rep.*, 202 (2003).
35. Eide, M., Olsen, A., Ninnemann, U.S., Eldevik, T. A global estimate of the full oceanic ¹³C Suess effect since the preindustrial *Glob. Biogeochem. Cycles* **31**, 492–514 (2017).
36. Lam, P., Kuypers, M.M.M. Microbial nitrogen cycling processes in oxygen minimum zones. *Ann. Rev. Mar. Sci.* **3**, 317-345 (2011).
37. Chance, R., Weston K., Alex R. Baker, A.R., Hughes, C., Malin, G., et al. Seasonal and interannual variation of dissolved iodine speciation at a coastal Antarctic site. *Mar. Chem.* **118**, 171-181(2010).
38. Spokes, L.J., Liss, P.L. Photochemically induced redox reactions in seawater, II. Nitrogen and iodide. *Mar. Chem.* **54**, 1-10 (1996).
39. Chance, R., Baker, A.R., Carpenter, L., Jickells, T.D. The distribution of iodide at the sea surface. *Environm. Sci. -Proc. Imp.* **16**, 1841- 1859 (2014).
40. Fairbanks, R.G., Sverdløve, M., Free, R., Wiebe, P.H., Bé, A.W.H. Vertical distribution and isotopic fractionation of living planktonic foraminifera in the Panama Basin. *Nature* **298**, 841-844 (1982).

41. Ravelo, A.C., Fairbanks, R.G. Oxygen isotopic composition of multiple species of planktonic foraminifera: recorders of modern photic zone temperature gradient. *Paleoceanography* **7**, 815-831 (1992).
42. Farmer, E.C., Kaplan, A., de Menocal, P.B., Lynch-Stieglitz, J. Corroborating ecological depth preferences of planktonic foraminifera in the tropical Atlantic with the stable isotope ratios of core top specimens. *Paleoceanography* **22**, doi:10.1029/2006PA001361 (2007).
43. Barker, S., Greaves, M., Elderfield, H. A study of cleaning procedures used for foraminiferal Mg/Ca paleothermometry. *G-cubed* **4**, 8407 (2003).
44. Altabet, M.A., Pilskahn, C., Thunell, R., Pride, C., Sigman, D., Chavez, F., Francois, R. The nitrogen isotope biogeochemistry of sinking particles from the margin of the Eastern North Pacific. *Deep-Sea Res. I* **46**, 655-679 (1999).
45. Deutsch, C., Sigman, D.M., Thunell, R.C., Meckler, A.N., Haug, G.H. Isotopic constraints on glacial/interglacial changes in the oceanic nitrogen budget. *Global Biogeochem. Cy.* **4**, 1-22 (2004).
46. Farrell, J.W., Pedersen, T.F., Calvert, S.E., Nielsen, B. Glacial-interglacial changes in nutrient utilization in the equatorial Pacific Ocean. *Nature* **377**, 514-517 (1995).
47. Robinson, R.S., Martinez, P., Pena, L.D., Cacho, I. Nitrogen isotope evidence for deglacial changes in nutrient supply in the eastern equatorial Pacific. *Paleoceanography* **24**, PA4213 (2009).
48. Rafter, P.A., Charles, C.D. Pleistocene equatorial Pacific dynamics inferred from the zonal asymmetry in sedimentary nitrogen isotopes. *Paleoceanography* **27**, PA3102 (2012).

49. Devol, A.H. Denitrification including Anammox. In Capone, D.G. et al. Eds. *Nitrogen in the Marine Environment* (2nd Edition), **pp 263-301** (2008).
50. Boyer, T.P., Antonov, J.I., Baranova, O., Coleman, C., Garcia, H.E., Grodsky, A., Johnson, D.R., Locarnini, R.A., Mishonov, A.V., O'Brien, T., Paver, C.R., Reagan, J.R., Seidov, D., Smolvar, I., Zweng, M.M. *World ocean database 2013. NOAA atlas NEDIS* 72. In Levitus, S. (Ed.), Silver Spring MD, **209 pp.** (2013).
51. Adkins, J.F., McIntyre, K., Schrag, D.P. The salinity, temperature and $\delta^{18}\text{O}$ of the glacial deep ocean. *Science* **298**, 1769-1773 (2002).
52. Debelius, B., Gómez-Parra, A., Forja, J.M. Oxygen solubility in evaporated seawater as a function of temperature and salinity. *Hydrobiologia* **632**, 157-165 (2009).

Data availability

Data generated during our study are available from <https://doi.pangaea.de/10.1594/PANGAEA.891185>.

Extended data figure and table captions

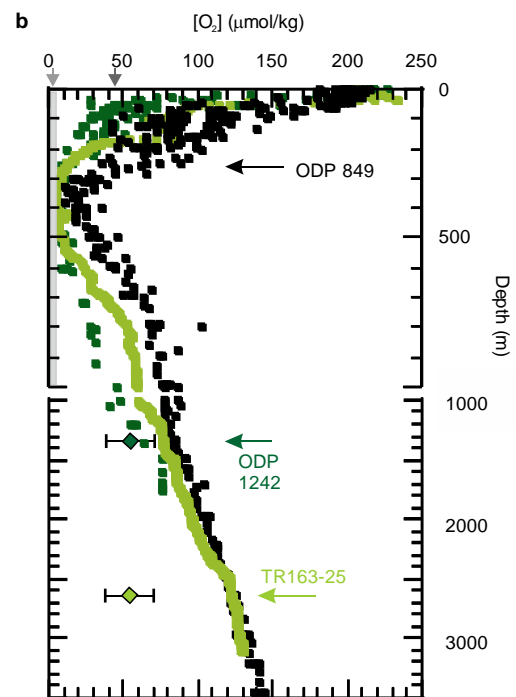
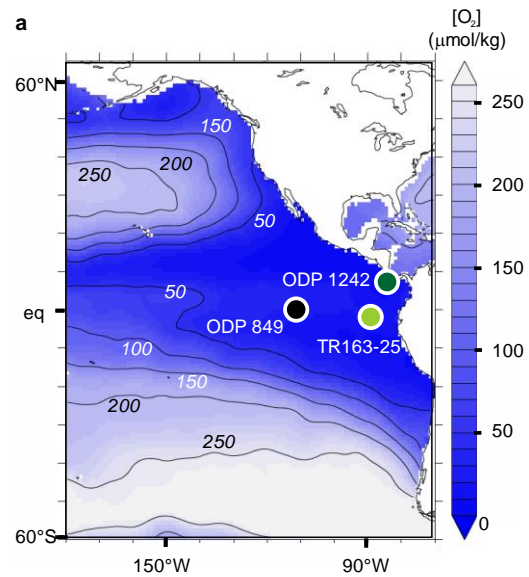
Extended data figure 1: Details of age models for ODP Sites 1242 and 849. **a** Matching of ODP 1242 benthic composite $\delta^{18}\text{O}$ record to the Pacific Intermediate water stacked $\delta^{18}\text{O}$ record of t^{24} , **b** matching ODP 849 benthic composite $\delta^{18}\text{O}$ record to Pacific deep water stacked $\delta^{18}\text{O}$ record of t^{24} .

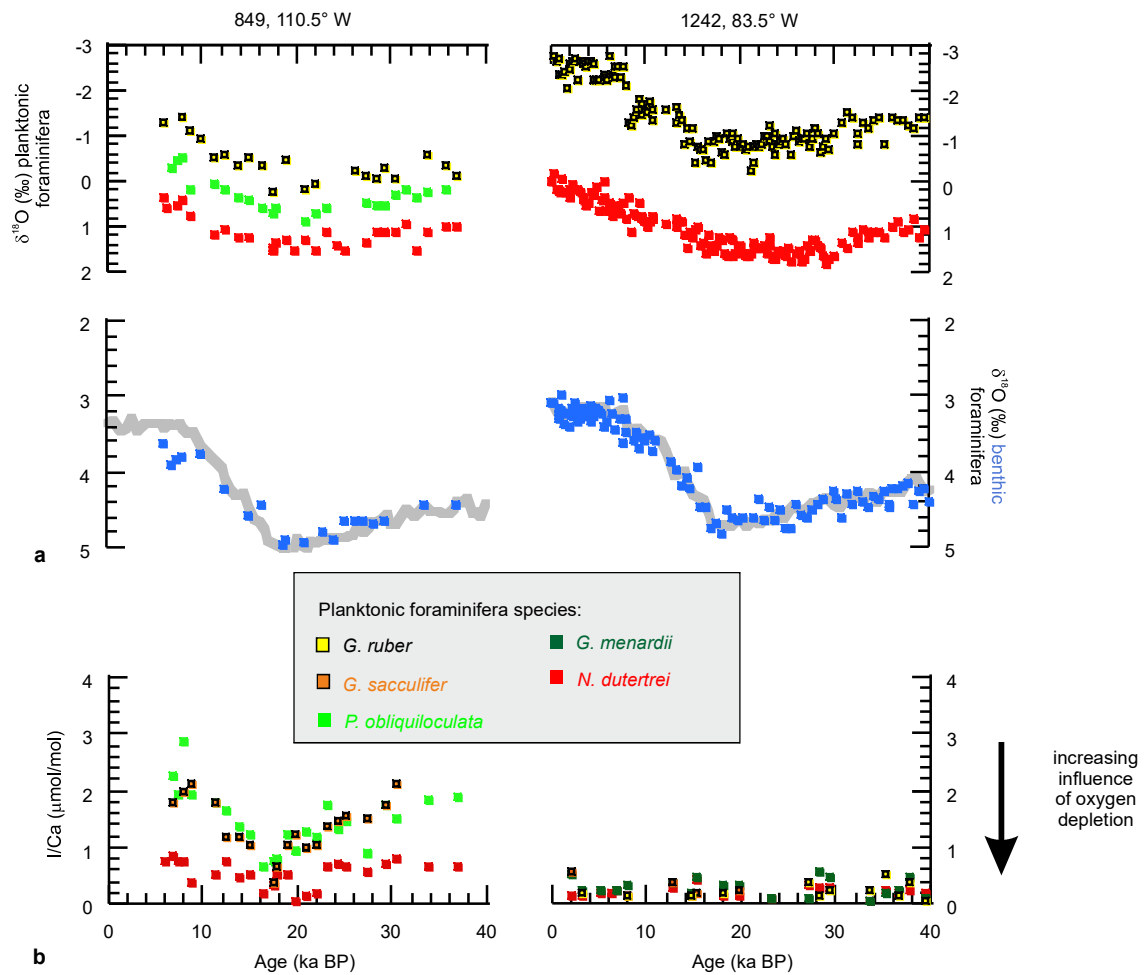
Extended data figure 2: Regional bulk sedimentary $\delta^{15}\text{N}$ records. Dark green: bulk sedimentary $\delta^{15}\text{N}$ record of ODP Site 1242⁴⁷; light green: bulk sedimentary $\delta^{15}\text{N}$ record of TR163-25 (this work); black: bulk sedimentary $\delta^{15}\text{N}$ record of ODP Site 849⁴⁸.

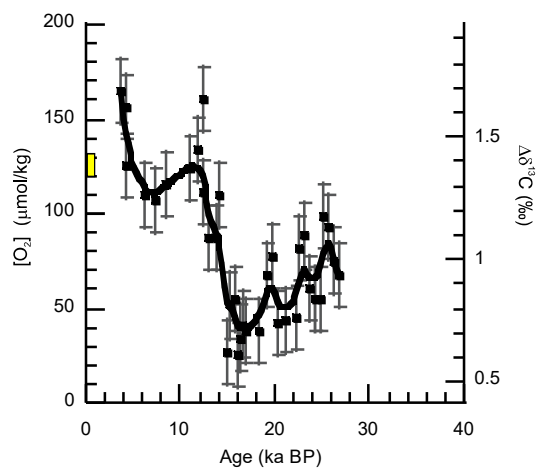
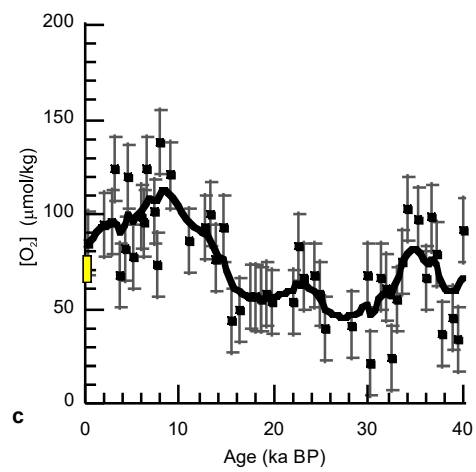
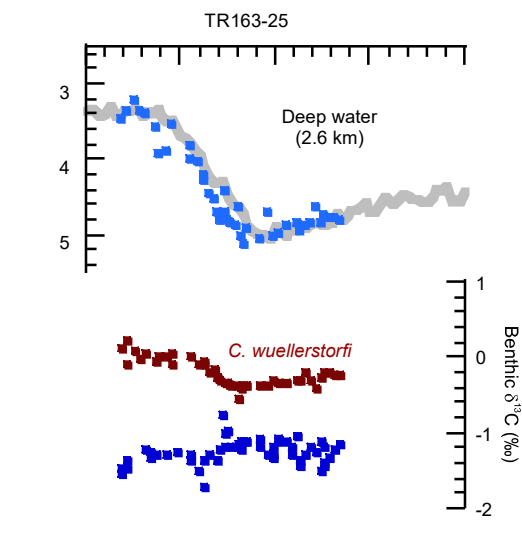
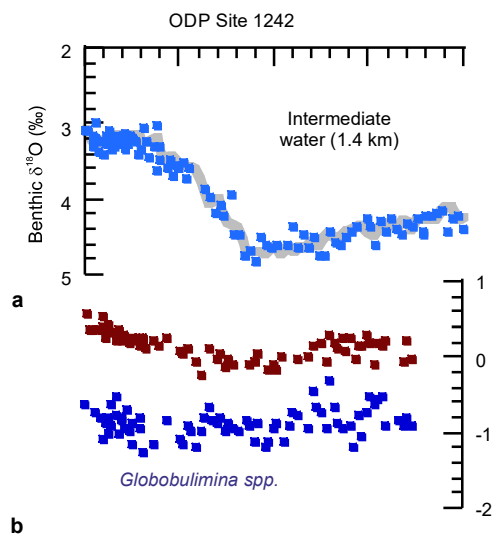
Extended data figure 3: Overview and LGM evolution of carbon isotopes and oxygen concentrations in the eastern tropical Pacific. **a** Dissolved oxygen concentrations (modern: dark blue: North Atlantic north of 50°N, light blue: South Atlantic south of 50°S, black/grey: Southeast/Southwest Pacific south of 50°S, dark purple/light purple: Northeast and Northwest Pacific north of 50°N; and reconstructed (last 40 kyr, dark green ODP Site 1242, mustard green TR163-25) plotted against carbon isotopes of DIC of seawater (‰) (data from^{22, 50} using <https://www.nodc.noaa.gov/OC5/SELECT/dbsearch/dbsearch.html>. Square boxes represent modern values at the two sites; diamonds represent LGM values (average 18-22 ka BP). **b** Latitudinal profile of the difference in Pacific carbon isotopes between the LGM (18-22 kyrs, from epifaunal benthic foraminifera) and recent (DIC) seawater carbon isotopes (extrapolated from³⁴). Inset: histogram of LGM- DIC $\delta^{13}\text{C}$ (waters deeper than 1.3 km) shows normal distribution (0.1 ‰ bin-width).

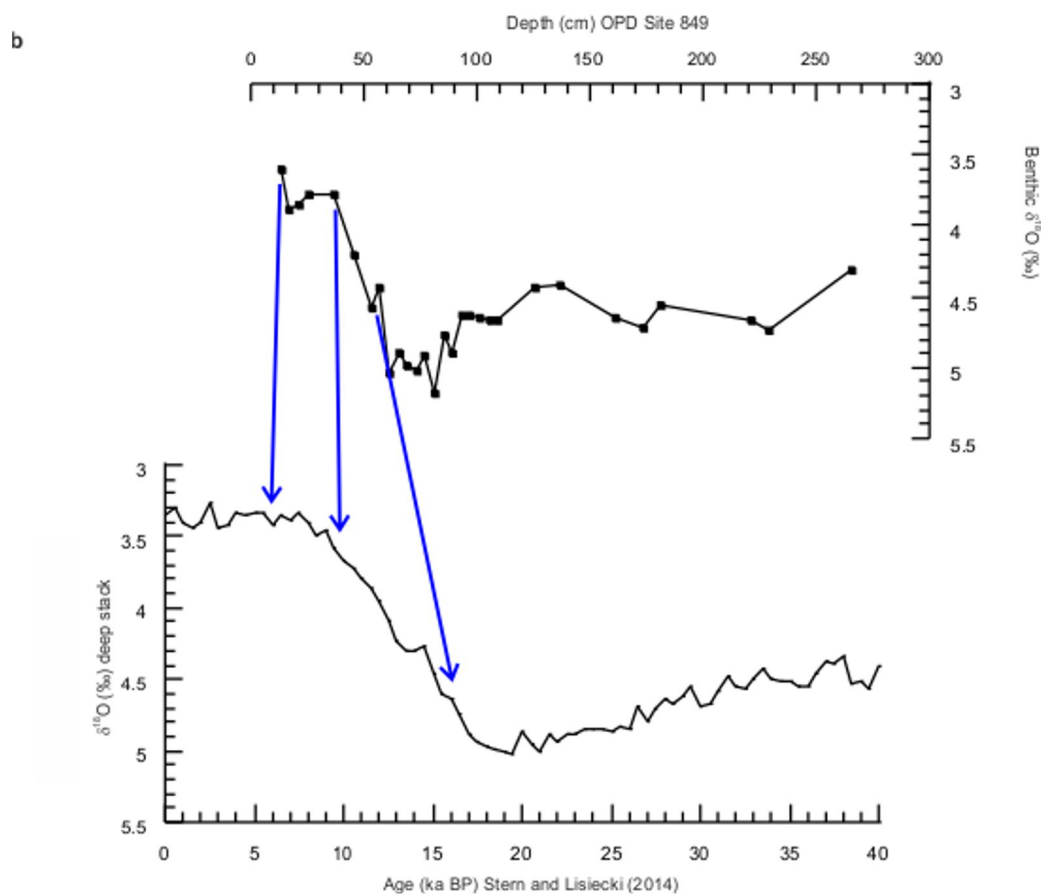
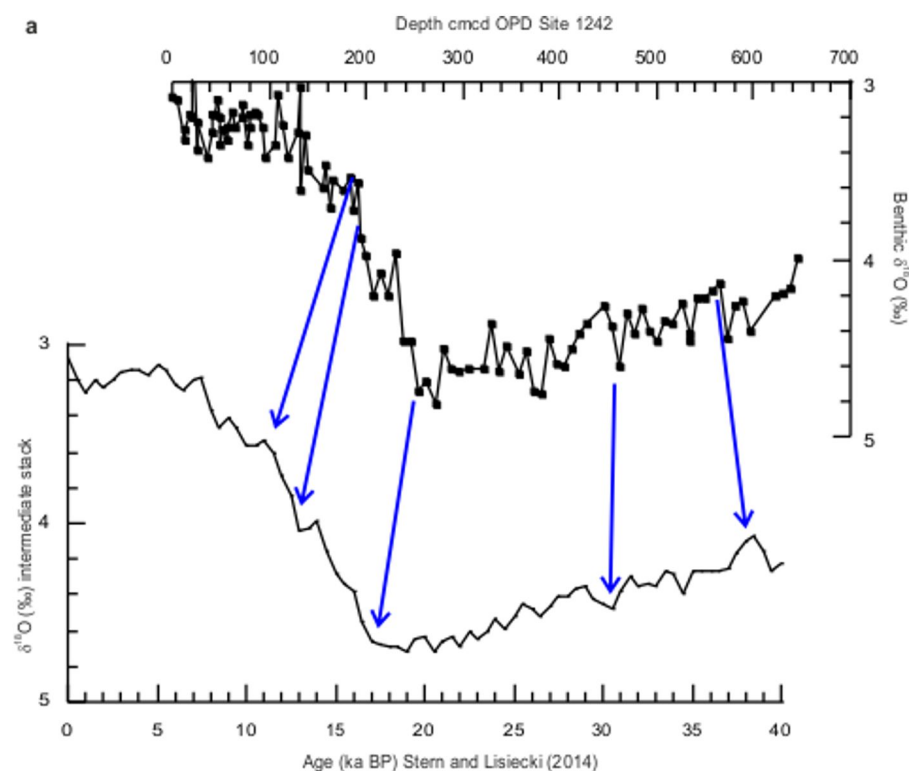
Extended data table 1: Age control points for ODP Site 1242 and 849. Based on matching the benthic foraminiferal composite oxygen isotope records with the stacked records of²⁴.

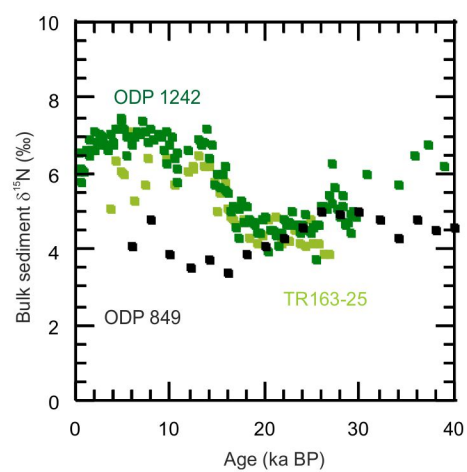
Extended data table 2: Age control points for TR163-25. Based on ^{14}C dates and calculated reservoir ages.

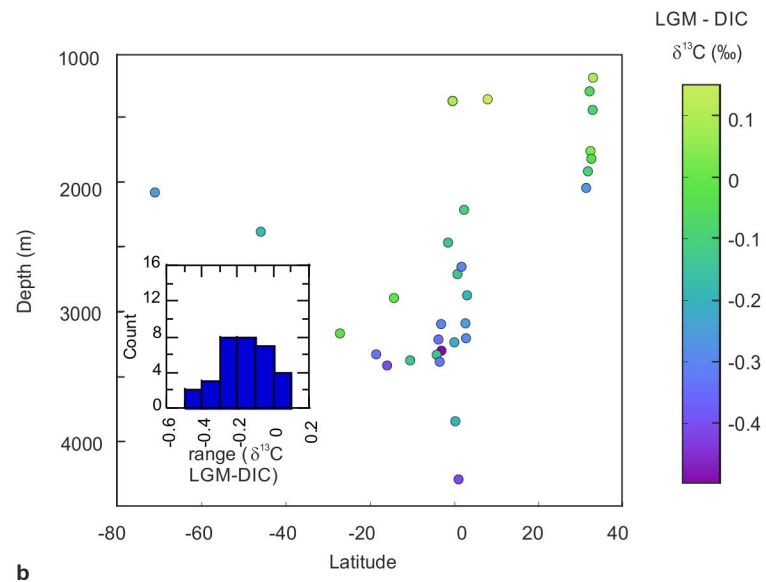
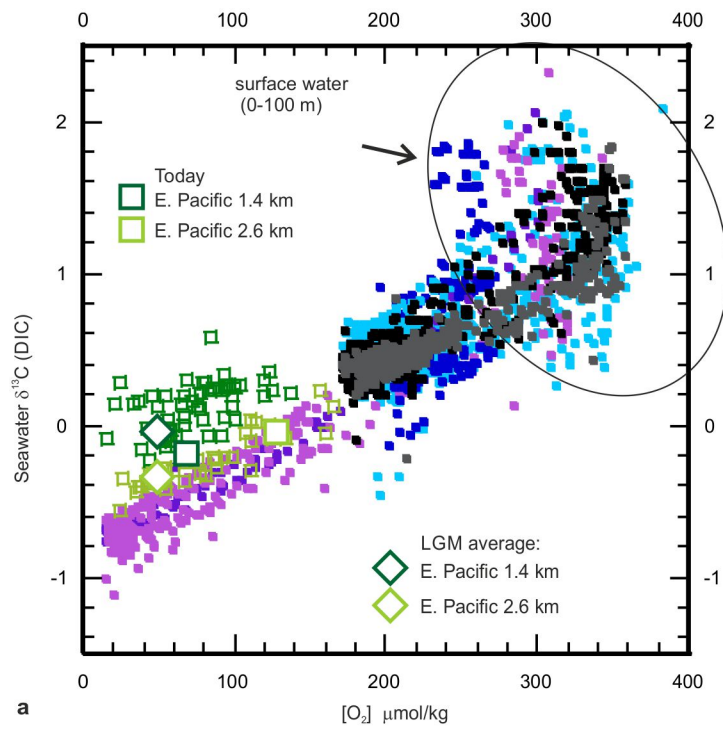












Depth (cm) 1242	Age (ka BP) 1242		Depth (cm) 849	Age (ka BP) 849
0	0		13	6
191	11		37	10
196	13		61	17.5
255	17			
461	30.5			
565	38			

TR163-25 depth (cm)	14C age (14C years)	Error $\pm 1\sigma$	ΔR	Species
40	7335	20	147 \pm 13	<i>G. ruber</i>
80	12895	45	1250 \pm 133	<i>N. dutertrei</i>
100	14250	60	1430 \pm 123	<i>N. dutertrei</i>
145	20850	130	2032 \pm 201	<i>N. dutertrei</i>